Asymptotic Giant Branch Stars
T. Le Bertre, A. Lèbre and C. Waelkens, eds.
I.A.U. Symposium 191, 1999

Diffraction-limited 76 mas speckle-masking interferometry of the carbon star IRC +10 216 and related AGB objects with the SAO 6 m telescope

G. Weigelt, T. Blöcker, K.-H. Hofmann, and R. Osterbart

Max-Planck-Institut für Radioastronomie, Auf dem Hügel 69, 53121 Bonn, Germany

Y.Y. Balega

Special Astrophysical Observatory, Nizhnij Arkhyz, Karachaevo-Cherkesia, 357147, Russia

A. J. Fleischer and J. M. Winters

Technische Universität Berlin, Institut für Astronomie und Astrophysik, 10623 Berlin, Germany

Abstract. We present high-resolution J-, H-, and K-band observations of the carbon star IRC +10 216. The images were reconstructed from 6 m telescope speckle interferograms using the speckle masking bispectrum method. The H image has the unprecedented resolution of 70 mas. The H and K images consist of at least five dominant components within a 0.21 arcsec radius and a fainter asymmetric nebula. The J–, H–, and K–band images seem to have an X-shaped bipolar structure. A comparison of our images from 1995, 1996, 1997, and 1998 shows that the separation of the two brightest components A and B increased from $\sim$193 mas in 1995 to $\sim$246 mas in 1998.

The cometary shapes of component A in the H and J images and the 0.79 μm and 1.06 μm HST images suggest that the core of A is not the central star, but the southern (nearer) lobe of the bipolar structure. The position of the central star is probably at or near the position of component B, where the H–K color has its largest value of H–K = 4.2.

If the star is located at or near B, then the components A, C, and D are located close to the inner boundary of the dust shell at separations of $\sim$200 mas $\sim$30 AU (projected distance) $\sim$6 stellar radii for a distance of $\sim$150 pc, in agreement with our 2-dimensional radiative transfer modelling.

In addition to IRC +10 216 we studied the stellar disks and the dust shells of several related objects. Angular resolutions of 24 mas at 700 nm or 57 mas 1.6 μm were achieved.

https://doi.org/10.1017/S0074180900203173 Published online by Cambridge University Press

1. Speckle masking observations of IRC +10 216

IRC +10 216 (CW Leo) is the nearest, brightest and best-studied carbon star. The central star of IRC +10 216 is a long-period variable with a period of about 650 days. Distance estimates between 110 pc and 170 pc were reported (see Crosas & Menten 1997 and references therein). High-angular-resolution IR observations of IRC +10 216 and of its circumstellar dust shell were reported by Dyck et al. (1991), Danchi et al. (1994), McCarthy et al. (1990), Christou et al. (1990), Osterbart et al. (1997), Weigelt et al. (1997, 1998), and Haniff & Buscher (1998). Recent detailed radiative transfer calculations for IRC +10 216 were presented by Groenewegen (1997).

The IRC +10 216 speckle interferograms were obtained with the 6 m telescope at the Special Astrophysical Observatory in Russia and our NICMOS 3 camera at four different epochs. The high-resolution J, H, and K images (Figs. 1 to 3) were reconstructed from the speckle interferograms using the speckle masking bispectrum method (Weigelt 1977, Lohmann et al. 1983, Weigelt 1991). The resolution of the J (April 2, 1996), H (January 23, 1997), and K (January 23, 1997) images are 149 mas, 70 mas, and 87 mas, respectively. We denote the resolved components in the H and K images as A, B, C, and D (in the order of decreasing peak intensity; Weigelt et al. 1998).

The separation of the components A and B was measured for four different epochs. The four obtained separations are: 193 mas (October 1995, phase 0.88), 201 mas (April 1996, phase 0.15), 212 mas (January 1997, phase 0.62), and 246 mas (June 98, phase 0.39). The linear regression fit gives a velocity for this motion of ~ 20 mas/yr. Assuming a distance of 150 pc (Crosas & Menten 1997) for IRC +10 216, this tangential velocity transforms to 14 km/s. This velocity is of the same order as the value of the radial expansion velocity of the circumstellar matter, 15 km/s (see Gensheimer & Snyder 1997 and references therein). From the present data there is no evidence that the motion inside the nebula is correlated with the stellar pulsation cycle.

2. Discussion

The core structure and the faint nebula in the H and K images. The multi-component structure of the IRC +10 216 K-band image (of the innermost 300 mas $\times$ 300 mas) has already been reported by Weigelt et al. (1998) and Haniff & Buscher (1998). This bright inner region is surrounded by a larger faint bipolar nebula (with $\sim 1\%$ of the peak brightness of A). On the northern side of this faint nebula two arms of the nebula can be seen at position angles of roughly 30°(NE) and 340°(NW) with respect to component A. On the southern side one arm is present at about 210°(SW). At 160°(counterside of the NW-arm) the nebula is much fainter. It may, therefore, be adequate to take the direction from component A to component B (about 20° position angle) as the direction of the main axis (see also Kastner & Weintraub 1994).

The bipolar J-band image. The J-band image (Fig. 1) and the 0.79 μm and 1.06 μm HST images (Haniff & Buscher 1998) show a bipolar structure of the nebula. The southern lobe has a cometary shape whereas the northern region of

https://doi.org/10.1017/S0074180900203173 Published online by Cambridge University Press

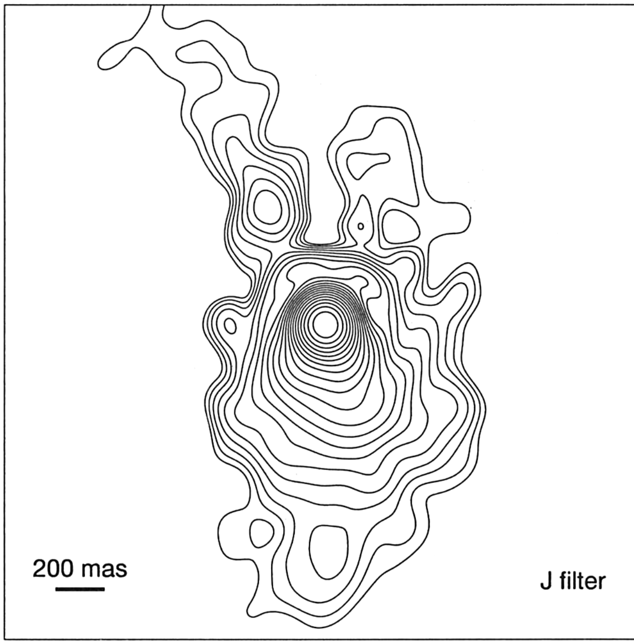

Figure 1. J–band image of IRC +10 216 with 149 mas resolution. In all images north is up and east to the left and the contour spacing is 0.25 mag.

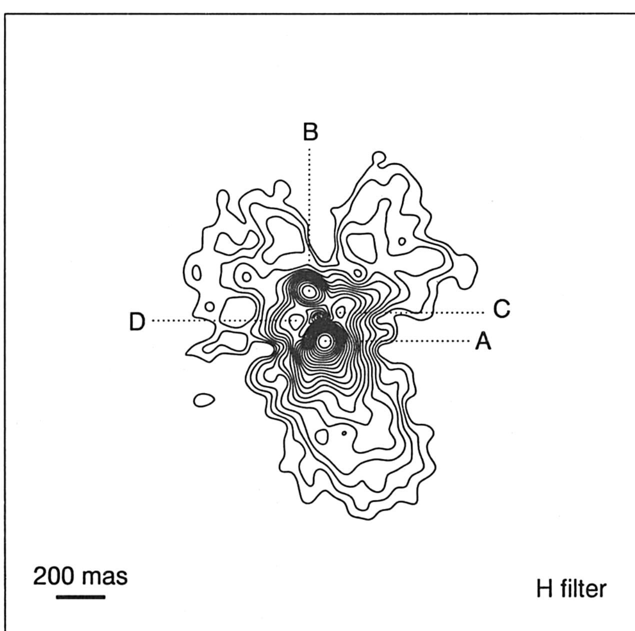

Figure 2. H–band image of IRC +10 216 with 70 mas resolution.

https://doi.org/10.1017/S0074180900203173 Published online by Cambridge University Press

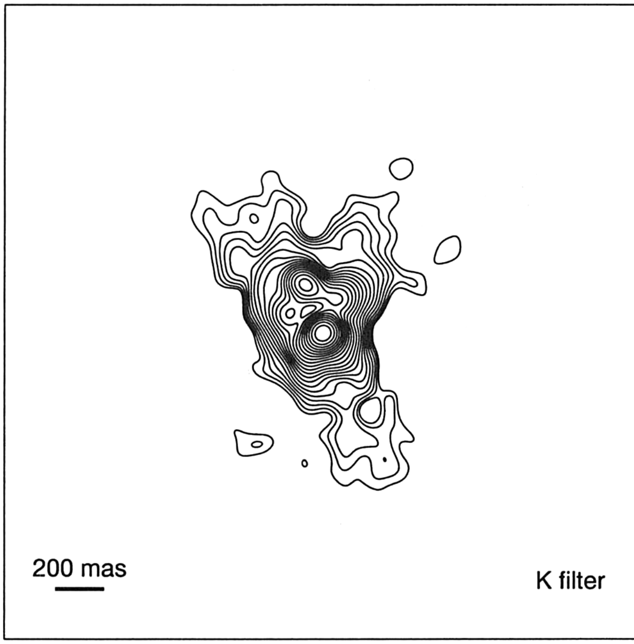

Figure 3. K–band image of IRC +10 216 with 87 mas resolution.

the images shows two arms reminiscent to (but much weaker than) the X–shaped structure of the Red Rectangle (see Men'shchikov et al. 1998).

H–K color image. In a square aperture of 1.6 arcsec the H and K magnitudes were determined to be K = 2.5 and H = 5.7. The integral color in this field is thus H–K = 3.2 ± 0.2. Our high–resolution H–K color image (Osterbart et al. 1999) shows that the components B, C, and D are rather red (H–K ≈ 4.2) in comparison with the integral color. The brightest component A (H–K = 3.2) as well as the *cometary* southern tails (H–K = 2 to 3) in the H and J image are bluer. These tails are a striking feature best seen in the high–resolution H–band image (Fig. 2). This structure and its relatively blue color suggest that component A is produced to a significant fraction by scattering of stellar light. This morphology can easily be understood under the assumption that the density of the dust shell is not sperically symmetric. The polar axis probably points with its southern side towards us. Component B may then be at or near the position of the star, strongly obscured and reddened by its environment. This suggests that the main axis of the nebula has a position angle of ∼ 20°.

Relative motion of A and B. The relative motion of the nebula components is clearly not related to the stellar variability which has a period of about 650 days. It may thus be related to either an overall expansion or a variability of the dust shell with a period significantly larger than the stellar pulsation period (cf. Winters et al. 1995).

Bipolar structure, clumpiness, and position of the central star. Theoretical models treating the dust formation mechanism in the envelope of long–period variable carbon stars (Winters et al. 1994a, b) predict that dust formation does

https://doi.org/10.1017/S0074180900203173 Published online by Cambridge University Press

not occur permanently but ceases regularly. Periods of this mechanism may be significantly different from the stellar pulsation period. This leads us to the conclusion that in our IRC +10 216 images we see the inner boundary of the dust shell moving outwards with approximately 15 km/s. The components in the central region of IRC +10 216 have separations of the order of only a few stellar radii and the travel time of newly formed dust over these distances is only a few years. The components A to D may be caused, for instance, by large convection cells in the stellar atmosphere leading to asymmetric and stochastic fluctuations of the dust formation and thus to disturbances of the overall bipolar geometry.

Consistent with preliminary results from our radiative transfer calculations (Men'shchikov et al. 1999, in preparation), the cometary shapes of A in the H and the J images and the 0.79 μm and 1.06 μm HST images (Haniff & Buscher 1998) suggest that the core of A is *not* the central star, but the central star is at or near B, between the northern and southern J–band lobes separated by $\sim$500 mas. B is very red (H–K$\approx$4.2) and, therefore, it is not visible in the J–band image. If the star is now at or near B, then the components A, C, D and the northern components in the J image are probably located at the inner boundary of the dust shell. The radiative transfer models imply that the polar axis is inclined by intermediate angles (roughly 50°) with respect to the plane of the sky.

3. Diffraction-limited speckle masking studies of R Cas, AFGL 2290, and the Red Rectangle

In addition to IRC +10 216 we have studied the wavelength dependence of the size and the shape of the Mira stars R Cas (Weigelt et al. 1996) and R Leo, the aspherical dust shell of the oxygen-rich AGB star AFGL 2290 (Gauger et al. 1999), and the bipolar structure of the Red Rectangle (Men'shchikov et al. 1998). One-dimensional radiative transfer modelling of AFGL 2290 and two-dimensional radiative transfer modelling of the Red Rectangle was used for the interpretation of the observations.

Acknowledgments. This research has made use of the SIMBAD database, operated at CDS, Strasbourg, France.

References

Christou J.C., Ridgway S.T., Buscher D.F., Haniff C.A., McCarthy D.W., 1990, in Astrophysics with infrared arrays, R. Elston (ed.), ASP Conf. Series 14, p. 133

Crosas M., Menten K.M., 1997, ApJ 483, 913

Danchi W.C., Bester M., Degiacomi C.G., Greenhill L.J., Townes C.H., 1994, AJ 107, 1469

Dyck H.M., Benson J.A., Howell R.R., Joyce R.R., Leinert C., 1991, AJ 102, 200

https://doi.org/10.1017/S0074180900203173 Published online by Cambridge University Press

Gauger A., Balega Y.Y., Irrgang P., Osterbart R., Weigelt G., 1999, High–resolution speckle masking interferometry and radiative transfer modeling of the oxygen–rich AGB star AFGL 2290, A&A, submitted

Gensheimer P.D., Snyder L.E., 1997, ApJ 490, 819

Groenewegen M.A.T., 1997, A&A 317, 503

Haniff C.A., Buscher D.F., 1998, A&A 334, L5

Kastner J.H., Weintraub D.A., 1994, ApJ 434, 719

Lohmann A.W., Weigelt G., Wirnitzer B., 1983, Appl. Opt. 22, 4028

McCarthy D.W., McLeod B.A., Barlow D., 1990, in Astrophysics with infrared arrays, R. Elston (ed.), ASP Conf. Series No. 14, p. 139

Osterbart R., Balega Y.Y., Weigelt G., Langer N., 1997, in Planetary Nebulae, H.J. Habing and H.J.G.L.M. Lamers (eds.), IAU Symposium 180, Kluwer Academic Press, Dordrecht, p. 362

Osterbart R., Balega Y.Y., Blöcker T., Men'shchikov A.B., Weigelt G., 1999, High–resolution bispectrum speckle interferometry of the bipolar dust shell around the carbon star IRC +10 216, in preparation

Men'shchikov A.B., Balega Y.Y., Osterbart R., Weigelt G., 1998, New Ast. 3, 601

Men'shchikov A.B., Balega Y.Y., Blöcker T., Osterbart R., Weigelt G., 1999, in preparation

Weigelt G., 1977, Optics Commun. 21, 55

Weigelt G., 1991, in Progress in Optics Vol. 29, E. Wolf (ed.), North Holland, Amsterdam, p. 293

Weigelt G., Balega Y.Y., Hofmann K.-H., Scholz M., 1996, A&A 316, L21

Weigelt G., Balega Y.Y., Hofmann K.-H., Langer N., Osterbart R., 1997, in Science with the VLT Interferometer, F. Paresce (ed.), Springer, Berlin, p. 206

Weigelt G., Balega Y.Y., Blöcker T., Fleischer A.J., Osterbart R., Winters J.M., 1998, A&A 333, L51

Winters J.M., Dominik C., Sedlmayr E., 1994a, A&A 288, 255

Winters J.M., Fleischer A.J., Gauger A., Sedlmayr E., 1994b, A&A 290, 623

Winters J.M., Fleischer A.J., Gauger A., Sedlmayr E., 1995, A&A 302, 483

https://doi.org/10.1017/S0074180900203173 Published online by Cambridge University Press